Journal of Visualized Experiments

A Semi-High-Throughput Adaptation of the NADH-Coupled ATPase Assay for Screening Small Molecule Inhibitors

--Manuscript Draft--

Article Type:	Invited Methods Article - JoVE Produced Video
Manuscript Number:	JoVE60017R1
Full Title:	A Semi-High-Throughput Adaptation of the NADH-Coupled ATPase Assay for Screening Small Molecule Inhibitors
Keywords:	ATPase assay, NADH, fluorescence, semi high-throughput screening, inhibitory constant, myosin
Corresponding Author:	Courtney Miller Scripps Research Institute Jupiter, FL UNITED STATES
Corresponding Author's Institution:	Scripps Research Institute
Corresponding Author E-Mail:	CMiller@scripps.edu
Order of Authors:	Laszlo Radnai
	Rebecca Stremel
	James Sellers
	Gavin Rumbaugh
	Courtney Miller
Additional Information:	
Question	**Response**
Please indicate whether this article will be Standard Access or Open Access.	Standard Access (US$2,400)
Please indicate the **city, state/province, and country** where this article will be **filmed**. Please do not use abbreviations.	Jupiter, FL

Cover Letter

Courtney A. Miller, Ph.D.

Associate Professor
Department of Molecular Medicine
Department of Neuroscience
The Scripps Research Institute, Florida

130 Scripps Way, 3B3
Jupiter, FL 33458-5284
Tel: 561-228-2958
Fax: 561-228-3059
Email: cmiller@scripps.edu

March 18, 2019

Dear Dr. Myers,

We are pleased to be submitting our manuscript, "A semi-high-throughput adaptation of the NADH-coupled ATPase assay for screening small molecule inhibitors," for consideration for publication in *JoVE*.

A nicotinamide adenine dinucleotide (NADH)-coupled ATPase assay has been adapted to semi-high throughput screening of small molecule myosin inhibitors. This kinetic assay is run in a 384 well microplate format with total reaction volumes of only 20µl per well. The platform should be applicable to virtually any ADP producing enzyme.

This manuscript has been read and approved by all listed authors.

Thank you for your consideration of our submission.

Sincerely,

TITLE:

A Semi-High-Throughput Adaptation of the NADH-Coupled ATPase Assay for Screening Small Molecule Inhibitors

AUTHORS AND AFFILIATIONS:

Laszlo Radnai[1,2], Rebecca F. Stremel[1,2], James R. Sellers[3], Gavin Rumbaugh[2], Courtney A. Miller[1,2]

[1]Department of Molecular Medicine, The Scripps Research Institute, Jupiter, FL, USA
[2]Department of Neuroscience, The Scripps Research Institute, Jupiter, FL, USA
[3]Laboratory of Molecular Physiology, NHLBI, National Institutes of Health, Bethesda, MD, USA

Corresponding author:
Courtney A. Miller (cmiller@scripps.edu)

Email addresses of co-authors:
Laszlo Radnai (lradnai@scripps.edu)
Rebecca F. Stremel (rstremel@scripps.edu)
James R. Sellers (sellersj@nhlbi.nih.gov)
Gavin Rumbaugh (grumbaug@scripps.edu)

KEYWORDS:

ATPase assay, NADH, fluorescence, semi high-throughput screening, inhibitory constant, myosin

SUMMARY:

A nicotinamide adenine dinucleotide (NADH)-coupled ATPase assay has been adapted to semi-high throughput screening of small molecule myosin inhibitors. This kinetic assay is run in a 384-well microplate format with total reaction volumes of only 20 µL per well. The platform should be applicable to virtually any ADP producing enzyme.

ABSTRACT:

ATPase enzymes utilize the free energy stored in adenosine triphosphate to catalyze a wide variety of endergonic biochemical processes in vivo that would not occur spontaneously. These proteins are crucial for essentially all aspects of cellular life, including metabolism, cell division, responses to environmental changes and movement. The protocol presented here describes a nicotinamide adenine dinucleotide (NADH)-coupled ATPase assay that has been adapted to semi-high throughput screening of small molecule ATPase inhibitors. The assay has been applied to cardiac and skeletal muscle myosin II's, two actin-based molecular motor ATPases, as a proof of principle. The hydrolysis of ATP is coupled to the oxidation of NADH by enzymatic reactions in the assay. First, the ADP generated by the ATPase is regenerated to ATP by pyruvate kinase (PK). PK catalyzes the transition of phosphoenolpyruvate (PEP) to pyruvate in parallel. Subsequently, pyruvate is reduced to lactate by lactate dehydrogenase (LDH), which catalyzes the oxidation of NADH in parallel. Thus, the decrease in ATP concentration is directly correlated to the decrease in NADH concentration, which is followed by change to the intrinsic fluorescence of NADH. As long as PEP is available in the reaction system, the ADP concentration remains very low, avoiding

inhibition of the ATPase enzyme by its own product. Moreover, the ATP concentration remains nearly constant, yielding linear time courses. The fluorescence is monitored continuously, which allows for easy estimation of the quality of data and helps to filter out potential artifacts (e.g., arising from compound precipitation or thermal changes).

INTRODUCTION:

Myosins are mechanochemical energy transducers that hydrolyze adenosine triphosphate (ATP) to generate directional movement along the filaments of the actin cytoskeleton in eukaryotes[1,2]. They have both structurally and kinetically adapted to their various intracellular functions, such as the transport of organelles, muscle contraction or the generation of cytoskeletal tension[1,2]. The myosin superfamily is represented by ~40 myosin genes belonging to ~12 distinct myosin classes in the human genome[3,4]. Members of the myosin classes play various roles in a highly diverse set of disorders, such as several cancers, neurological disorders, skeletal myopathies, and hypertrophic cardiomyopathy[5,6]. Given the large number of physiological and pathological functions of these molecular motors, it is not surprising that they are becoming increasingly recognized as drug targets for a variety of conditions[7]. Significant progress has been made recently in the discovery of new myosin inhibitors[8-10] and activators[11], and to improve the properties of existing ones[12-15].

The nicotinamide adenine dinucleotide (NADH)-coupled ATPase assay has long been used to measure the ATPase activity of various enzymes, such as the sarcoplasmic reticulum Ca^{2+} pump ATPase[16], the DNA repair ATPase Rad54[17], the AAA+ ATPase p97[18] or the microtubule motor kinesin[19]. The assay employs an ATP regeneration cycle. The adenosine diphosphate (ADP) generated by the ATPase is regenerated to ATP by pyruvate kinase (PK), which transforms one molecule of phosphoenolpyruvate (PEP) to pyruvate in parallel. Subsequently, pyruvate is reduced to lactate by lactate dehydrogenase (LDH). That, in turn, oxidizes one molecule of NADH to NAD. Therefore, the decrease in NADH concentration as a function of time equals the ATP hydrolysis rate. The ATP regeneration cycle keeps the ATP concentration nearly constant and the ADP concentration low as long as PEP is available. This results in linear time courses, making it simple to determine the initial reaction rates and helps to avoid product inhibition by ADP[19]. Although the NADH-coupled ATPase assay has already been adapted to a 96-well format[20], the high reaction volumes (~150 µL) make it relatively expensive due to the high demand of reagents, rendering it less amenable to rapid screening of large numbers of compounds. Alternative methods, such as the malachite green assay[19,21], which relies on the detection of the phosphate produced by the ATPase enzyme, were proven more suitable for miniaturization and high-throughput screening[22-24]. However, an endpoint assay is more likely to be affected by several artifacts (discussed below), which may remain undiscovered in the absence of full-time courses.

Here, the NADH-coupled ATPase assay has been optimized for semi-high throughput screening of small molecule inhibitors. Skeletal and cardiac muscle myosin II's and the myosin inhibitors blebbistatin[8], *para*-aminoblebbistatin[13] and *para*-nitroblebbistatin[12] are used to demonstrate the power of the assay, which relies on NADH fluorescence as a readout. This protocol is amenable to screening projects focused on any ADP producing enzymes.

PROTOCOL:

1. Preparing stock solutions and reagents

1.1. Prepare dithiothreitol (DTT) stock solution by dissolving crystalline DTT in distilled water to a final concentration of 1000 mM. Adjust the pH to 7.0 with 1 M NaOH solution. Aliquot and store at -20 °C.

1.2. Prepare ATP stock solution by dissolving crystalline ATP in distilled water to a final concentration of 100 mM. Adjust the pH to 7.0 with 1 M NaOH solution. Aliquot and store at -20 °C.

1.3. Prepare 10x NADH buffer containing 70 mM 3-(N-morpholino)propanesulfonic acid (MOPS), 10 mM $MgCl_2$, 0.9 mM ethylene glycol-bis(β-aminoethyl ether)-N,N,N′,N′-tetraacetic acid [EGTA], and 3 mM NaN_3. Adjust the pH to 7.0 with 1 M NaOH solution. Store at 4 °C.

1.4. Prepare 1x myosin buffer containing 10 mM MOPS and 0.1 mM EGTA. Adjust the pH to 7.0 with 1 M NaOH solution. Store at 4 °C. Add bovine serum albumin (BSA) and DTT to a final concentration of 0.1% (w/v%) and 1 mM, respectively, before use.

1.5. Prepare 1x actin buffer containing 4 mM MOPS, 0.1 mM EGTA, 2 mM $MgCl_2$, and 3 mM NaN_3. Adjust the pH to 7.0 with 1 M NaOH solution. Store at 4 °C. Add BSA and DTT to a final concentration of 0.1% (w/v%) and 1 mM, respectively, before use.

1.6. Prepare NADH stock solution by dissolving crystalline NADH in 10x NADH buffer to a final concentration of 5.5 mM. Aliquot and store at -20 °C.

1.7. Prepare PEP stock solution by dissolving crystalline PEP in 10x NADH buffer to a final concentration of 50 mM. Aliquot and store at -20 °C.

1.8. Prepare LDH stock solution by dissolving lyophilized LDH powder in a mixture of glycerol and 10x NADH buffer (50%:50%) to a final concentration of 2000 U/mL. Centrifuge the solution to remove any undissolved protein present (7,197 x *g*, 20 °C, 10 min). Transfer the supernatant into a clean centrifuge tube carefully. Aliquot and store at -20 °C.

1.9. Prepare PK stock solution by dissolving lyophilized PK powder in a mixture of glycerol and 10x NADH buffer (50%:50%) to a final concentration of 10000 U/mL. Centrifuge the solution to remove any undissolved protein present (7,197 x *g*, 20 °C, 10 min). Transfer the supernatant into a clean centrifuge tube carefully. Aliquot and store at -20 °C.

1.10. Reconstitute the lyophilized cardiac and skeletal muscle myosin II samples by adding 100 µL distilled water to obtain 10 mg/mL stock solutions corresponding to ~37.9 µM and ~40.8 µM myosin concentrations (monomeric), respectively. For further details, see manufacturer's instructions.

1.11. Prepare F-actin from rabbit muscle acetone powder as described by Pardee and Spudich[25].

2. Measuring ATPase activities and inhibitory effects of small molecule inhibitors

2.1. Prepare compound plate.

2.1.1. Dissolve compounds of interest in high-quality dimethylsulfoxide (DMSO).

2.1.2. Create fifteen-step serial 1:2 dilutions starting from 10 mM compound concentration in DMSO.

2.1.3. Transfer the samples to a 384-well polypropylene plate in triplicates (12.5 µL each) using a multichannel pipette. Use two rows on the compound plate for one compound (instead of three columns) to minimize the number of wells potentially affected by edge effects. Use the last three wells in the second row for each compound as negative control (DMSO only). Do not use the first and the last row on the plate for compound dilutions.

2.1.4. Transfer pure DMSO into the wells of the first row (reserved for NADH calibration).

2.1.5. Use the last row for positive control.

NOTE: *Para*-aminoblebbistatin at 4 mM concentration in DMSO was used here.

2.2. Prepare 4500 µL of 20 µM diluted actin solution for each assay plate (384-well black-wall polystyrene microplate). Mix the solution thoroughly by pipetting up and down 30x using a 5 mL pipette to reduce viscosity and heterogeneity by breaking actin filaments. Centrifuge the solution to remove any precipitated protein present (7,197 x *g*, 20 °C, 10 min). Carefully transfer the supernatant into a clean centrifuge tube.

2.3. Prepare master mix containing LDH and PK enzymes ("enzyme mix"). For each assay plate, combine 171.4 µL of LDH solution, 171.4 µL of PK solution and 3189.3 µL or 3252.9 µL of myosin buffer for assays involving cardiac or skeletal muscle myosin II's, respectively, in a 15 mL conical centrifuge tube. Do not add any myosin at this point to avoid aggregation and precipitation.

2.4. Prepare master mix containing all substrates ("substrate mix"). For each plate, combine 162.1 µL of ATP, 162.1 µL of PEP and 324.1 µL of NADH solution in a 15 mL conical centrifuge tube. Do not add actin at this point to avoid aggregation and precipitation.

2.5. Create seven-step serial 1:2 dilutions of NADH for calibration starting from 250 µM.

2.5.1. Mix 12.3 µL of NADH stock solution with 257.7 µL of myosin buffer in a 1.5 mL microcentrifuge tube.

2.5.2. Aliquot 135 µL of myosin buffer into seven 1.5 mL microcentrifuge tubes.

2.5.3. Transfer 135 µL of solution from the first tube into the second and mix by pipetting. Repeat until reaching the 7^{th} tube.

2.5.4. Use the last tube as no-NADH control (buffer only).

2.6. Using an 8-channel pipette, transfer 20 µL of the NADH calibration solutions into the first row of the assay plate in triplicates.

2.7. Add 68 µL of cardiac or 4.2 µL of skeletal muscle myosin II to the enzyme mix. Vortex briefly.

2.8. Except the first row, dispense 8.4 µL of enzyme mix into each well of the assay plate.

2.9. Transfer 100 nL of solutions from the compound plate to the assay plate containing enzyme mix using an automated liquid handling system equipped with a 100 nL pin tool head.

2.10. Shake the assay plate for 1 min at room temperature at 1200 rpm using a microplate shaker.

2.11. Add 4,052 µL of actin to the substrate mix. Vortex briefly.

2.12. Dispense 11.6 µL of substrate mix into each well of the assay plate (except first row) to start the enzymatic reaction.

2.13. Shake the assay plate for 1 min at room temperature at 1200 rpm using a microplate shaker.

2.14. Centrifuge the assay plate at 101 x *g* for 30 s.

2.15. Make sure that the inner temperature of the plate reader has been stabilized at 25 ˚C. Load the plate and shake for another 30 s. This shaking step is necessary to make the shape of the liquid surface similar in each well and allows time for the plate to reach measurement temperature.

2.16. Record NADH fluorescence for 30 min scanning the plate in 45 s intervals. Use a 380 nm, 10 nm bandwidth excitation filter and a 470 nm, 24 nm bandwidth emission filter in conjunction with a 425 nm cut-off dichroic mirror. Run the measurement in high-concentration mode. Optimize the number of flashes, detector gain, plate dimensions and measurement height before running the assays.

NOTE: Final assay conditions are 300 nM cardiac/20 nM skeletal muscle myosin II, 10 µM actin, 40 U/mL LDH, 200 U/mL PK, 220 µM NADH, 1 mM PEP, 1 mM ATP in a buffer containing 10 mM MOPS (pH = 7.0), 2 mM $MgCl_2$, 0.15 mM EGTA, 0.1 mg/mL BSA, 0.5% (v/v) DMSO and 1 mM DTT. The total volume is 20 µL/well. The highest final compound concentration is 50 µM. 20 µM *para*-aminoblebbistatin in 0.5% DMSO serves as the positive control and 0.5% DMSO alone is the

negative control. All measurements are carried out in triplicates.

3. Analyzing data

3.1. Plot the observed fluorescence intensity against time for each well.

3.2. Perform simple linear regression to determine the slope and intercept of the fluorescence responses for each well. The slope is proportional to the ATP (NADH) consumption rate, while the intercept is proportional to the NADH concentration at the beginning of the measurement (t = 0 s).

3.3. Construct a calibration curve for NADH by plotting the intercepts obtained for the first row of the plate against the concentration of NADH. Make sure that the intercepts depend linearly on the NADH concentration.

NOTE: The intercepts estimate the real fluorescence intensities at t = 0 s with much more confidence than the average of the raw fluorescence intensity reads at t ≈ 0 s.

3.4. Perform simple linear regression to obtain the slope and intercept of the NADH calibration line.

NOTE: The intercept describes the fluorescence background signal (no NADH present), while the slope corresponds to the extrapolated/theoretical fluorescence intensity of a 1 M NADH solution in that particular experiment.

3.5. Divide the slope of the fluorescence response obtained for the rest of the wells by the slope of the NADH calibration line to convert fluorescence changes to ATP consumption rates.

3.6. Plot the ATP consumption rates against the concentration of the inhibitor.

3.7. To determine inhibitory constants, use appropriate statistical software to fit the dose-response data to the following quadratic equation corresponding to a simple one-to-one binding equilibrium model:

$$Y = Y_{min} + (Y_{max} - Y_{min}) \frac{K_I + [E]_t + [I]_t - \sqrt{(K_I + [E]_t + [I]_t)^2 - 4[E]_t[I]_t}}{2[E]_t},$$

where Y is the ATP consumption rate, Y_{min} is the ATP consumption rate int the absence of inhibitor, Y_{max} is the theoretical ATP consumption rate at 100% inhibition, K_I is the inhibitory constant, $[E]_t$ and $[I]_t$ are the total concentration of the enzyme (myosin) and inhibitor, respectively.

REPRESENTATIVE RESULTS:

The typical plate layout map used for screening experiments is shown in **Figure 1**. The first and

last rows are reserved for NADH calibration and positive control (20 µM *para*-aminoblebbistatin, 0.5% DMSO), respectively. The remaining rows (B to O) are used to test the inhibitory activity of compounds. Here, fifteen-step serial 1:2 dilutions starting from 10 mM compound concentration in DMSO are prepared and transferred from the compound plate to the assay plate, such that the highest final compound concentration is 50 µM (in 0.5% DMSO) on the assay plate. Two rows are used to obtain a dose-response curve for one compound (48 datapoints/compound). Note that the plate layout maps can be re-designed to support the specific aims of a given project. For example, if the goal were to obtain single-point screening data for a large number of compounds, one could test 112 compounds on a single 384-well plate using the same layout for positive control and NADH calibration (calculating with triplicates for each compound). It is always advised to have a minimum of 3 datapoints for one compound (or for each concentration) and to avoid using only the wells along the edges of the plate for one compound, as these datapoints may be influenced by edge effects. To estimate the importance of edge effects, always run a full plate with negative control only first.

The fluorescence intensities have a linear dependence on the concentration of NADH as shown in **Figure 2A**. The slope of the linear fit is used during data analysis to convert fluorescence changes to reaction rates. Note that the raw fluorescence intensity trace obtained for each well of the NADH calibration is analyzed by linear regression first (a similar analysis is shown in **Figure 2B,C** for compound data). These traces are expected to show exponential decay over time due to photobleaching of the fluorophore. However, photobleaching is very slow and therefore, the raw data can be analyzed by linear fits. The slope and intercept of these fits correspond to the initial rate of photobleaching and the fluorescence intensity at t = 0 s, respectively. The intercepts of these linear fits are used instead of the average of the raw fluorescence reads at t = 0 s to construct the NADH calibration curve because the intercepts are estimated based on more data and, therefore, the associated errors are much smaller.

Figure 2B,C demonstrates that regardless of the myosin used or the presence of the inhibitor, the time courses are linear in the time window of the measurements. The highest (50 µM) and lowest (0 µM) inhibitor concentrations here correspond to ~100% and 0% inhibition, respectively. Note that due to the amount of raw data, the actual analysis would appear chaotic if shown on a single panel. Therefore, these panels have been simplified to better visualize the process. The average of the raw fluorescence intensity reads was calculated for all of the parallel experiments (triplicates for each concentration) and converted to NADH concentrations here. Only 3 inhibitor concentrations are shown. In the real analysis, each raw fluorescence intensity trace (48/compound tested) is analyzed by linear regression first, and subsequently, the slopes are converted to ATP consumption rates.

It is always advisable to demonstrate that the reaction rates change linearly with the enzyme concentration, as shown in **Figure 2D** and **Figure 2E** for skeletal and cardiac muscle myosin II's, respectively. Based on the linear fits, the final assay concentration of the enzyme can be easily estimated. For example, a reaction rate of ~5 x 10^{-8} Ms^{-1} is recommended for 30-min time courses. If an activator is used in the reaction mixtures (such as actin here), it is recommended to run the experiments both in the presence and absence of the activator to ensure that the

expected effect (activation) is present. The conditions and the procedure must follow the final protocol as closely as possible. Here, a dilution series of myosin was prepared in myosin buffer in eight microcentrifuge tubes first. Subsequently, a mix of LDH and PK enzymes were added. Finally, the reactions were started by adding substrate mix to each tube in parallel, using a multichannel pipette. Reaction mixes were immediately transferred to one row of the assay plate in triplicates. If actin was absent, actin buffer was used instead. No other parameters were changed (see the note of step 2.16 in the protocol for final assay conditions).

Figure 2F shows ATP consumption rates obtained for multiple negative and positive control reactions (half plate each). These data can be compared based on the Z` value or "screening window coefficient"[26], which is a widely used statistical parameter to estimate the quality of high-throughput assays. It compares the positive and negative controls by taking both the means and the standard deviations into account:

$$Z` = \frac{3(\sigma_n + \sigma_p)}{|\mu_n - \mu_p|},$$

where σ_n, σ_p and μ_n, μ_p are the standard deviations and means of the negative and positive controls, respectively. The two populations are well separated if the Z` value falls between 0.5 and 1. A Z` = 0.78 obtained here shows that the assay can be considered as excellent[26].

To demonstrate that the assay can be used to determine inhibitory constants, the small molecule myosin inhibitor blebbistatin[8] and two analogues, *para*-nitroblebbistatin[12] and *para*-aminoblebbistatin[13] have been chosen here, as shown in **Figure 3A** and **Figure 3B**. Blebbistatin is an uncompetitive, allosteric myosin inhibitor[27,28]. One molecule of blebbistatin binds to one motor domain of myosin and blocks the ATPase cycle by stabilizing the myosin-ADP-phosphate complex[27,28]. Therefore, the inhibitory effects of blebbistatin derivatives was modelled using a simple, one-to-one binding model here (see step 3.7 in the protocol). Note that this model may not have been applicable if the ATP consumption rates had not shown linear dependency on myosin concentration (see **Figure 2D,E**). The kinetic aqueous solubility of blebbistatin, *para*-nitroblebbistatin and *para*-aminoblebbistatin has been reported to be 426 µM, 3.6 µM and 9.3 µM, respectively[13]. No abnormalities in the signal were observed at or below the reported solubilities in our experiments; however, several artifacts appeared when either blebbistatin or *para*-nitroblebbistatin was used above their reported solubility values, as shown in **Figure 4**. Therefore, the signal recorded at concentrations higher than the solubility was excluded from the data analysis in these cases. *Para*-aminoblebbistatin is highly soluble, and therefore, solubility was not a limiting factor in that case.

Finally, it is always recommended to test whether the inhibitory effects of any positive hits are specific to the target ATPase enzyme. The coupled reaction system employs two other enzymes, LDH and PK, and inhibition of one of these would result in a false positive signal. Running the ATPase assay with an unrelated ATPase enzyme may help to filter out these false positive hits (for further recommendations, see discussion). *Para*-aminoblebbistatin and apyrase, an ATP hydrolyzing enzyme producing ADP and inorganic phosphate[29], were used here as an example to

demonstrate such a control experiment, as shown in **Figure 5**.

FIGURE LEGENDS:

Figure 1: Assay plate layout. Seven-step serial 1:2 dilutions of NADH starting from 250 µM concentration is prepared and subsequently dispensed into row A in triplicate for calibration (black to green color gradient). The last three wells of row A contain myosin buffer only (no NADH control, white). The last row (P) is used for the positive control (20 µM *para*-aminoblebbistatin; red). A typical dose-response experiment requires two rows (e.g., B and C). Therefore, 7 dose-response experiments can be run in parallel on a single 384-well plate (represented by blue to white color gradients). Every sample is loaded as triplicates. Here, the highest final compound concentrations start at 50 µM (in 0.5% DMSO). The last three wells of every second row are reserved for the negative control (no compound, 0.5% DMSO only; cyan).

Figure 2: Representative ATPase data. (**A**) A two-fold dilution series of NADH was prepared and transferred into the first row of each measurement plate. Fluorescence intensity was recorded for 30 min and the raw data was analyzed by simple linear regression. The intercept of each regression line was plotted against the concentration of NADH. Note that in an ideal case, the fluorescence intensity at t = 0 s could simply be used to obtain the calibration line. However, while the raw fluorescence data is very noisy, the intercepts give an accurate estimate of the fluorescence intensity at t = 0 s and their associated standard error (shown as error bars) is very small. (**B**,**C**) Representative fluorescence intensity traces of the skeletal (**B**) and cardiac (**C**) muscle myosin II ATPase reactions were recorded in the presence of various levels (see insets) of *para*-aminoblebbistatin. For simplicity, data points and error bars represent the average of three independent measurements and the associated standard deviation, respectively. Simple linear regression was performed (solid lines) to obtain reaction rates. Note that a typical dose-response experiment is comprised of 15 different inhibitor concentrations and negative control in triplicates on the measurement plate (see **Figure 1**) and the linear regression is performed individually for each fluorescence intensity trace. For simplicity, only 3 different concentrations are shown here. (**D**,**E**) Basal (red) and actin-activated (blue) ATPase rates were determined for various skeletal (**D**) and cardiac (**E**) muscle myosin II concentrations. The ATPase rates show linear dependency on the myosin concentration. (**F**) Positive (red) and negative (blue) controls (half plate each) were run in parallel on a 384-well assay plate and the Z-factor (Z`) was calculated to assess the quality of the ATPase assay. A Z' value of 0.78 indicates a reliable assay with very well separated positive and negative controls.

Figure 3: Dose-response curves and analysis of inhibitory constants. Cardiac (**A**) and skeletal (**B**) muscle myosin II's were used to test the inhibitory activity of blebbistatin, *para*-aminoblebbistatin and *para*-nitroblebbistatin. ATPase rates (blue) were obtained by applying simple linear regression to the raw fluorescence data. Error bars represent the standard error of fitting and were used as weighting factors during fitting a quadratic equation (see step 3.7 in the protocol) representing a simple equilibrium binding model (red). Data obtained above solubility was influenced by artifacts and excluded from analysis.

Figure 4: Solubility-related artifacts. (**A**) Fluorescence intensity traces for blebbistatin obtained in an ATPase assay using skeletal muscle myosin II show linearly decreasing signal depending on the amount of inhibitor present (blue). However, when blebbistatin was used above solubility (50 μM initial blebbistatin concentration), an increase in the signal was observed (red), most likely due to the formation of brightly fluorescent blebbistatin crystals[13]. (**B**) In the case of *para*-nitroblebbistatin, which is a non-fluorescent analog of blebbistatin[12], the raw fluorescence intensity traces appeared normal (decreasing). However, the highest level of inhibition was much lower than expected (based on the positive control). Therefore, only the reaction rates obtained below solubility (blue) were included in data analysis. Reaction rates obtained above solubility (red) diverge from the determined dose-response curve (green), as precipitation limits the amount (concentration) of the inhibitor remaining in solution.

Figure 5: Inhibitory effects of *para*-aminoblebbistatin in skeletal muscle myosin II and apyrase ATPase assays. *Para*-aminoblebbistatin inhibited skeletal muscle myosin II with a K_I of 1.7 μM, while no inhibition was detected when apyrase[29] was used as an ATPase in the same coupled reaction system. This experiment clearly demonstrates that *para*-aminoblebbistatin is specific to myosin and does not inhibit PK or LDH, thus the detected inhibitory effect is not an artifact. Apyrase was used at 0.5 nM concentration. No myosin or actin was present, and the reaction was performed in a buffer containing 100 mM MOPS (pH = 7.0), 3 mM $CaCl_2$, 2 mM $MgCl_2$, 3 mM NaN_3, 1 mM DTT, and 0.1% BSA. No other modifications were made to the protocol.

DISCUSSION:

Critical steps in the protocol

Optimize plate layout by running several plates with negative control only (ATPase reaction with no inhibitor). Inspect the results carefully for patterns in reaction rates. For example, these may arise from edge effects and/or imperfections in the hydrophilic surface coating of “non-binding” plates. If a pattern is observed, change plate type and/or plate layout to minimize the artifacts. For example, a typical dose-response curve (16 concentrations with triplicates, 48 points total) can be either arranged in three columns or two rows on a 384-well plate. These arrangements yield 6 and 4 datapoints, respectively, that are likely affected by edge effects. Therefore, the row arrangement is always preferred.

Modifications and troubleshooting

Note that the observed fluorescence responses must be linear throughout the full time-course of the reaction. Non-linearities may occur in the first few minutes due to thermal changes or in the last few minutes due to reaching equilibrium. If non-linearities are present, one can either adjust reaction parameters (e.g., dilute myosin, change measurement temperature) or simply limit the analysis to the linear part of the data.

Non-linearities may also be present at the beginning of the reactions if the binding of the inhibitor to the ATPase enzyme is slow (occurring over minutes). In this case, the reaction is expected to

slow down over time as the enzyme-inhibitor complex accumulates. Incubate the assay plate before adding the substrate mix as necessary to avoid this problem.

The assay conditions must be chosen in such a way that the linear part of reactions is longer than 15 minutes. Shorter linear parts correspond to less useful datapoints (<20, as the scanning of the whole plate takes ~45 seconds). Therefore, the linear fits yield less reliable slopes (reaction rates) with much higher standard errors. On the other hand, it is not recommended to obtain kinetic reads longer than ~120 minutes. Such experiments might be affected by protein denaturation or concentration changes due to solvent evaporation. These criteria can be met most easily by adjusting the myosin concentration.

It is important to ensure that the reactions catalyzed by PK and LDH are not rate limiting in the coupled reaction system. Control experiments performed without the ATPase of interest or at high levels of a potent ATPase inhibitor would show no (or little) activity. However, the addition of ADP would result in a quick signal decrease if LDH and PK are active and work correctly. The rate of NADH consumption is expected to be very high in this control experiment, so it is crucial to start detection as soon as possible after the reaction has been initiated by the addition of ADP.

It is always recommended to exclude any observed ATPase rates obtained above the solubility of the inhibitor from the data analysis. As the solubility depends on the temperature, purity of the compound, and differences in the composition of the solution, it is highly recommended to measure it under conditions that are highly similar to the actual conditions (temperature, buffer, etc.) under which the ATPase assay is carried out. Attempting to use small molecule inhibitors above solubility may result in precipitation that could influence the results (see **Figure 4**). Precipitation limits the concentration of the compound at or near solubility. Therefore, the ATPase rates cannot be reduced further by adding more inhibitor. Using a good positive control that shows ~100% inhibition, therefore, can help to identify such anomalies in the signal, even if the solubility is unknown. A large difference between the observed reaction rate of the positive control and the reaction rate belonging to the maximal inhibition level (I_{max}) determined by fitting is always a good indication of the problem. Gradually excluding more and more data from the analysis and/or using the positive control as I_{max} and keeping it fixed during the fitting process until a better fit is obtained is recommended in such cases. Inhibitor precipitation might also result in strong light scattering and may also change the optical properties of the inhibitor, leading to abnormally high observed signal intensities at the beginning of reactions and/or increasing signals over time. Raw data must always be carefully inspected, and the affected concentrations must be excluded from the analysis.

Limitations of the method

The final assay concentration for ATPases with a low turnover number (e.g., cardiac muscle myosin II) must be high (several hundred nM) to achieve measurable reaction rates within time window of the assay (30−120 minutes). Therefore, it might be important to use the quadratic binding model for the analysis of dose-response curves. Other binding models (hyperbolic, Hill) are typically not suitable for the analysis of such data. Moreover, the concentration of the ATPase

sets a lower limit to the range of measurable inhibitory constants because the dose response curves get indistinguishable in practice due to the presence of experimental errors if the K_I is close to or less than the concentration of the ATPase.

Differences in compound potencies should always be quantified by performing dose-response experiments and determining the inhibitory constants. Although single point screening data reflects these differences in theory, the non-linearity of the responses, together with the experimental error would make it extremely difficult to perform such an analysis. Single point screening experiments should be designed to capture even the relatively weak inhibitors with high confidence by choosing an appropriate inhibitor concentration and a pre-defined threshold response level to distinguish between active and inactive compounds.

Establishing that the differences between the inhibitory constants are statistically significant is best performed by re-writing the equation for nonlinear regression to determine pK_I ($-\log K_I$) instead of K_I, as pK_I is normally distributed, while K_I is not[30]. The uncertainty for pK_I is symmetrical, while it is not symmetrical for K_I[31]. Confidence intervals can be calculated for pK_I and t-test or analysis of variance (ANOVA) can be used to determine if the means of pK_I measurements are significantly different. However, caution must be taken when performing such statistical test as they assume homoscedasticity (same variance of data in groups). One can expect higher variance associated with pK_I when a full dose-response curve cannot be obtained due to compound solubility issues. In this case, other appropriate statistical tests not assuming equal variances (e.g., Welch's t-test) should be used.

Any compound inhibiting PK or LDH would give a false positive signal in the NADH-coupled ATPase assay. Some of these false positives can be identified by running the assay with an unrelated ADP producing enzyme. In this case, no inhibition for real positive hits can be expected, unless the inhibitor is an ATP analogue binding to both enzymes. To demonstrate such an analysis, we performed an ATPase assay using *para*-aminoblebbistatin and apyrase, an ATP hydrolyzing enzyme not related to myosines (see **Figure 5**). Alternatively, a different functional assay specific to the enzyme of interest, or a different ATPase assay not employing PK and LDH can be run to distinguish between real and false positive hits (e.g., the malachite green assay).

Measurement and analysis of the kinetics of the fluorescence intensity in all wells require a plate reader fast enough to scan the whole plate in less than ~90−60 seconds.

Significance of the method with respect to existing/alternative methods

Opposed to the "traditional" absorbance-based readout[16-20], the modified NADH-coupled ATPase assay presented here relies on NADH fluorescence. This makes the assay more sensitive, allowing the user to reduce excitation light intensity and thereby protect NADH or the inhibitors against photochemical decomposition.

Although the assay has been generally considered as not suitable for handling large number of samples[32], the small reaction volumes achieved here (20 µL) in a 384-well format makes it

amenable for semi-high throughput screening applications, especially if the determination of inhibitory constants is considered.

Alternative methods usually rely on the detection of the inorganic phosphate produced by the ATPase enzyme. For example, [γ-32P]ATP can be used as a substrate for the ATPase and subsequently, the liberated inorganic phosphate can be measured based on its radioactivity. The assay is sensitive; however, it requires the handling of radioactive substances and the remaining ATP must be separated from the inorganic phosphate (e.g., by adsorption of ATP on charcoal)[33]. In the above-mentioned malachite green assay, phosphate reacts with molybdate under acidic conditions and the resulting phosphomolybdate complex binds the malachite green dye causing a shift in its absorption spectrum[19,21-24]. This method also requires quenching of the ATPase reaction; therefore, it is mostly used as an endpoint-assay, especially in high throughput format. In contrast to the continuous monitoring of the ATPase reaction in the NADH-coupled assay, an endpoint assay simply assumes linear time courses and cannot reveal artifacts leading to non-linearities. Compounds interacting with malachite green or the complex formed may also lead to artifacts[21]. Moreover, the malachite green assay is very sensitive to phosphate contamination[24]. In contrast, the NADH-coupled assay is not sensitive to ADP contamination as ADP (which is always present at various levels in ATP samples) is quickly transformed to ATP by PK at the beginning of the reaction. There is no need for quenching or separation of the products. Another fluorometric assay for the measurement of ATPase rates has already been developed by coupling the ATP hydrolysis to the reaction catalyzed by nucleoside phosphorylase[34]. However, that assay does not utilize an ATP regeneration cycle, therefore the determination of initial reaction rates can be much more challenging.

Future applications or directions of the method

Many enzymes relying on ATPase activity have been explored as potential drug targets. These include cytoskeletal motor proteins belonging to the kinesin[35] and dynein families[36] and the DNA helicases[37], all of which are the terminal effectors in diverse signaling pathways. The assay described here can be easily optimized for drug discovery and development projects involving any enzyme catalyzing a reaction in which ADP is a product.

ACKNOWLEDGMENTS:
This work was supported by a grant from the National Institute of Neurological Disorders and Stroke and National Institute on Drug Abuse NS096833 (CAM).

DISCLOSURES:
The authors have nothing to disclose.

REFERENCES:
1. Heissler, S. M., Sellers, J. R. Kinetic Adaptations of Myosins for Their Diverse Cellular Functions. *Traffic.* **17** (8), 839-859 (2016).
2. Hartman, M. A., Spudich, J. A. The myosin superfamily at a glance. *Journal of Cell Science.* **125** (Pt 7), 1627-1632 (2012).

572 3. Berg, J. S., Powell, B. C., Cheney, R. E. A millennial myosin census. *Molecular Biology of the Cell.*
573 **12** (4), 780-794 (2001).
574 4. Sebe-Pedros, A., Grau-Bove, X., Richards, T. A., Ruiz-Trillo, I. Evolution and classification of
575 myosins, a paneukaryotic whole-genome approach. *Genome Biology and Evolution.* **6** (2), 290-
576 305 (2014).
577 5. Newell-Litwa, K. A., Horwitz, R., Lamers, M. L. Non-muscle myosin II in disease: mechanisms
578 and therapeutic opportunities. *Disease Models & Mechanisms.* **8** (12), 1495-1515 (2015).
579 6. He, Y. M., Gu, M. M. Research progress of myosin heavy chain genes in human genetic diseases.
580 *Yi Chuan.* **39** (10), 877-887 (2017).
581 7. Rauscher, A. A., Gyimesi, M., Kovacs, M., Malnasi-Csizmadia, A. Targeting Myosin by
582 Blebbistatin Derivatives: Optimization and Pharmacological Potential. *Trends in Biochemical*
583 *Sciences.* **43** (9), 700-713 (2018).
584 8. Straight, A. F. et al. Dissecting temporal and spatial control of cytokinesis with a myosin II
585 Inhibitor. *Science.* **299** (5613), 1743-1747 (2003).
586 9. Sirigu, S. et al. Highly selective inhibition of myosin motors provides the basis of potential
587 therapeutic application. *Proceedings of the National Academy of Sciences of the United States of*
588 *America.* **113** (47), E7448-E7455 (2016).
589 10. Green, E. M. et al. A small-molecule inhibitor of sarcomere contractility suppresses
590 hypertrophic cardiomyopathy in mice. *Science.* **351** (6273), 617-621 (2016).
591 11. Morgan, B. P. et al. Discovery of omecamtiv mecarbil the first, selective, small molecule
592 activator of cardiac Myosin. *ACS Medicinal Chemistry Letters.* **1** (9), 472-477 (2010).
593 12. Kepiro, M. et al. para-Nitroblebbistatin, the non-cytotoxic and photostable myosin II inhibitor.
594 *Angewandte Chemie International Edition.* **53** (31), 8211-8215 (2014).
595 13. Varkuti, B. H. et al. A highly soluble, non-phototoxic, non-fluorescent blebbistatin derivative.
596 *Scientific Reports.* **6**, 26141 (2016).
597 14. Verhasselt, S. et al. Discovery of (S)-3'-hydroxyblebbistatin and (S)-3'-aminoblebbistatin: polar
598 myosin II inhibitors with superior research tool properties. *Organic and Biomolecular Chemistry.*
599 **15** (9), 2104-2118 (2017).
600 15. Verhasselt, S., Roman, B. I., Bracke, M. E., Stevens, C. V. Improved synthesis and comparative
601 analysis of the tool properties of new and existing D-ring modified (S)-blebbistatin analogs.
602 *European Journal of Medicinal Chemistry.* **136**, 85-103 (2017).
603 16. Warren, G. B., Toon, P. A., Birdsall, N. J., Lee, A. G., Metcalfe, J. C. Reconstitution of a calcium
604 pump using defined membrane components. *Proceedings of the National Academy of Sciences*
605 *of the United States of America.* **71** (3), 622-626 (1974).
606 17. Kiianitsa, K., Solinger, J. A., Heyer, W. D. Rad54 protein exerts diverse modes of ATPase activity
607 on duplex DNA partially and fully covered with Rad51 protein. *Journal of Biological Chemistry.*
608 **277** (48), 46205-46215 (2002).
609 18. Hanzelmann, P., Schindelin, H. Structural Basis of ATP Hydrolysis and Intersubunit Signaling
610 in the AAA+ ATPase p97. *Structure.* **24** (1), 127-139 (2016).
611 19. Hackney, D. D., Jiang, W. Assays for kinesin microtubule-stimulated ATPase activity. *Methods*
612 *in Molecular Biology.* **164**, 65-71 (2001).
613 20. Kiianitsa, K., Solinger, J. A., Heyer, W. D. NADH-coupled microplate photometric assay for
614 kinetic studies of ATP-hydrolyzing enzymes with low and high specific activities. *Analytical*
615 *Biochemistry.* **321** (2), 266-271 (2003).

21. Carter, S. G., Karl, D. W. Inorganic phosphate assay with malachite green: an improvement and evaluation. *Journal of Biochemical and Biophysical Methods.* **7** (1), 7-13 (1982).
22. Henkel, R. D., VandeBerg, J. L., Walsh, R. A. A microassay for ATPase. *Analytical Biochemistry.* **169** (2), 312-318 (1988).
23. Rowlands, M. G. et al. High-throughput screening assay for inhibitors of heat-shock protein 90 ATPase activity. *Analytical Biochemistry.* **327** (2), 176-183 (2004).
24. Rule, C. S., Patrick, M., Sandkvist, M. Measuring In Vitro ATPase Activity for Enzymatic Characterization. *Journal of Visualized Experiments.* (114), 54305 (2016).
25. Pardee, J. D., Spudich, J. A. Purification of muscle actin. *Methods in Cell Biology.* **24**, 271-289 (1982).
26. Zhang, J. H., Chung, T. D., Oldenburg, K. R. A Simple Statistical Parameter for Use in Evaluation and Validation of High Throughput Screening Assays. *Journal of Biomolecular Screening.* **4** (2), 67-73 (1999).
27. Kovacs, M., Toth, J., Hetenyi, C., Malnasi-Csizmadia, A., Sellers, J. R. Mechanism of blebbistatin inhibition of myosin II. *Chem Journal of Biological Chemistry.* **279** (34), 35557-35563 (2004).
28. Allingham, J. S., Smith, R., Rayment, I. The structural basis of blebbistatin inhibition and specificity for myosin II. *Nature Structural & Molecular Biology.* **12** (4), 378-379 (2005).
29. Kettlun, A. M. et al. Purification and Characterization of 2 Isoapyrases from Solanum-Tuberosum Var Ultimus. *Phytochemistry.* **31** (11), 3691-3696 (1992).
30. Hulme, E. C., Trevethick, M. A. Ligand binding assays at equilibrium: validation and interpretation. *British Journal of Pharmacology.* **161** (6), 1219-1237 (2010).
31. Motulsky, H. J., Neubig, R. R. Analyzing binding data. *Current Protocols in Neuroscience.* **52** (1), 7.5.1-7.5.65 (2010).
32. Sehgal, P., Olesen, C., Moller, J. V. ATPase Activity Measurements by an Enzyme-Coupled Spectrophotometric Assay. *Methods in Molecular Biology.* **1377**, 105-109 (2016).
33. Solinger, J. A., Lutz, G., Sugiyama, T., Kowalczykowski, S. C., Heyer, W. D. Rad54 protein stimulates heteroduplex DNA formation in the synaptic phase of DNA strand exchange via specific interactions with the presynaptic Rad51 nucleoprotein filament. *Journal of Molecular Biology.* **307** (5), 1207-1221 (2001).
34. Banik, U., Roy, S. A continuous fluorimetric assay for ATPase activity. *Biochemistry Journal.* **266** (2), 611-614 (1990).
35. Xiao, Y. X., Yang, W. X. KIFC1: a promising chemotherapy target for cancer treatment? *Oncotarget.* **7** (30), 48656-48670 (2016).
36. See, S. K. et al. Cytoplasmic Dynein Antagonists with Improved Potency and Isoform Selectivity. *ACS Chemical Biology.* **11** (1), 53-60 (2016).
37. Datta, A., Brosh, R. M., Jr. New Insights Into DNA Helicases as Druggable Targets for Cancer Therapy. *Frontiers in Molecular Biosciences.* **5**, 59 (2018).

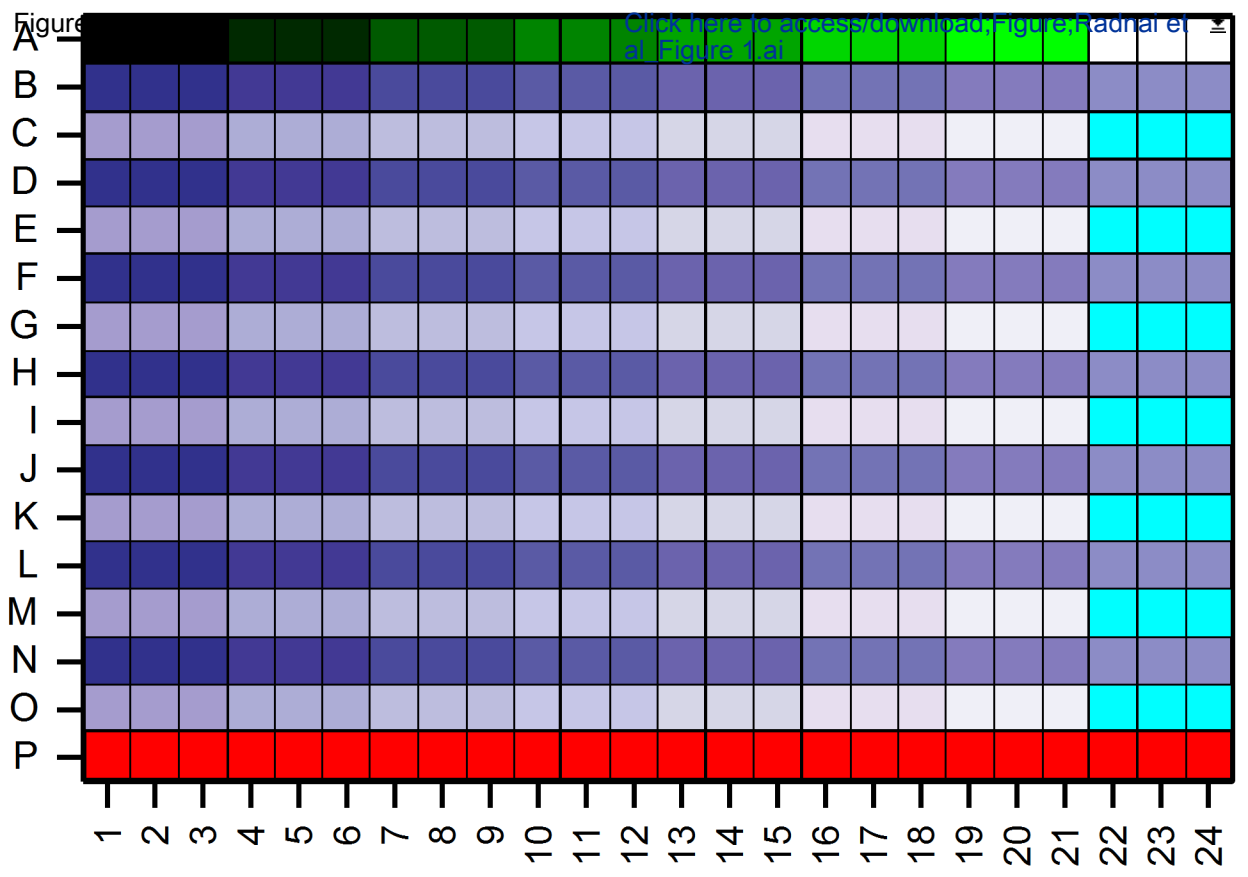
Figure
Click here to access/download;Figure;Radnaa et al_Figure 1.ai
A
B
C
D
E
F
G
H
I
J
K
L
M
N
O
P
1
2
3
4
5
6
7
8
9
10
11
12
13
14
15
16
17
18
19
20
21
22
23
24

Figure 2

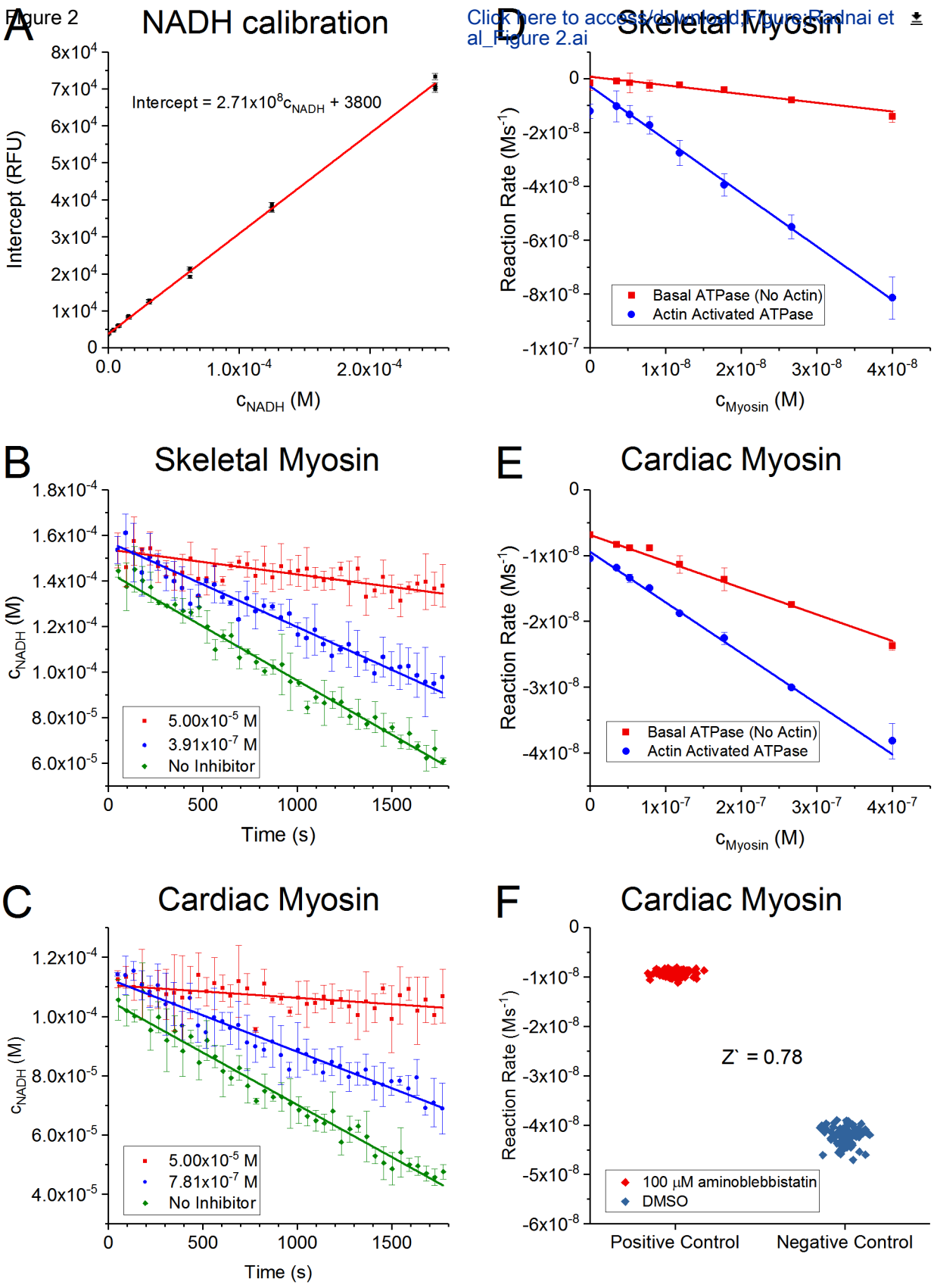

Figure 3

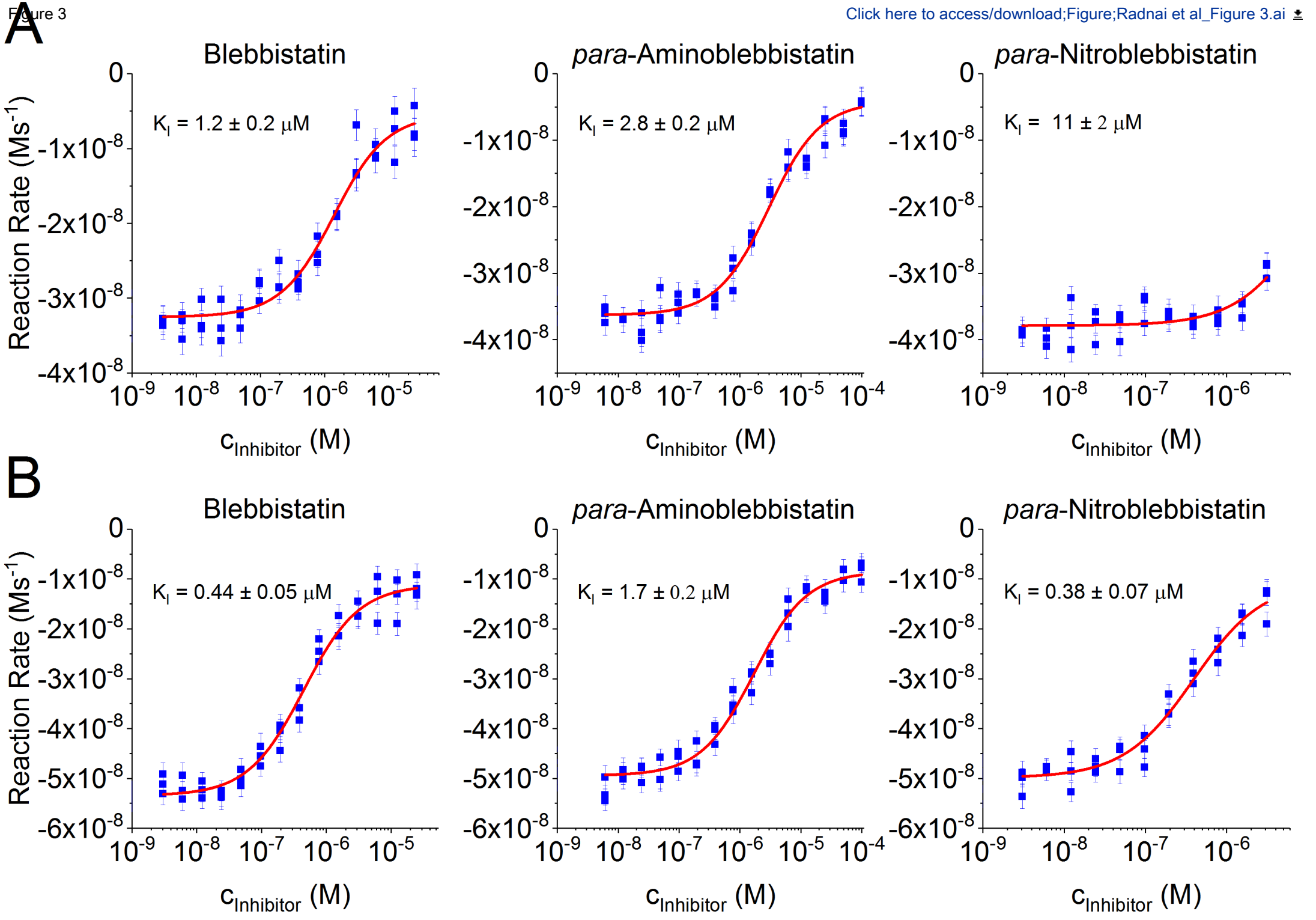

Figure 4

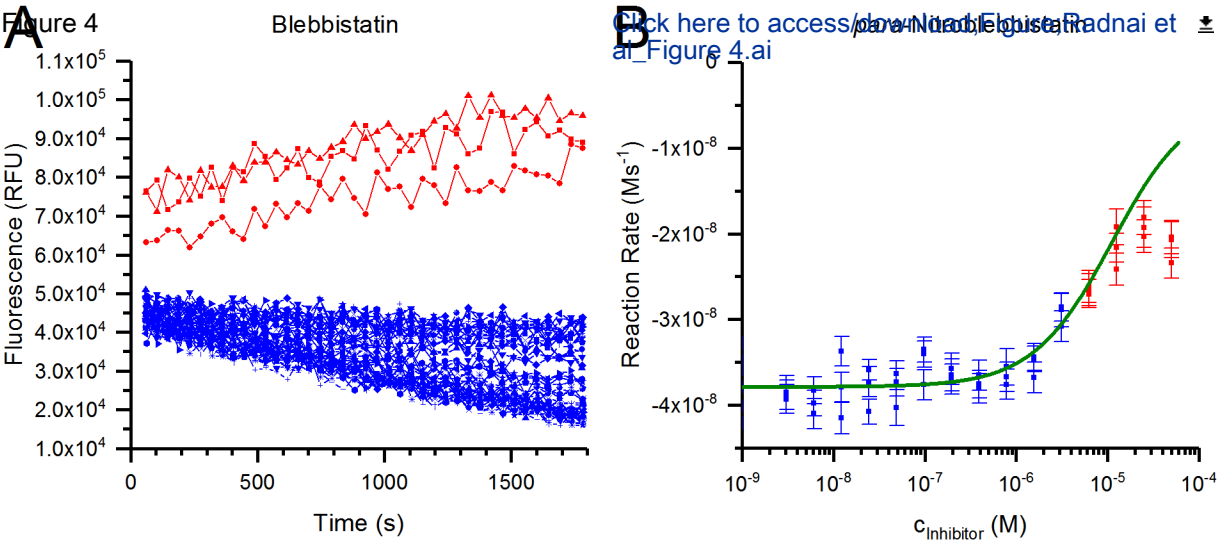

Figure 5

Click here to access/download;Figure;Radnai et al_Figure 5.ai

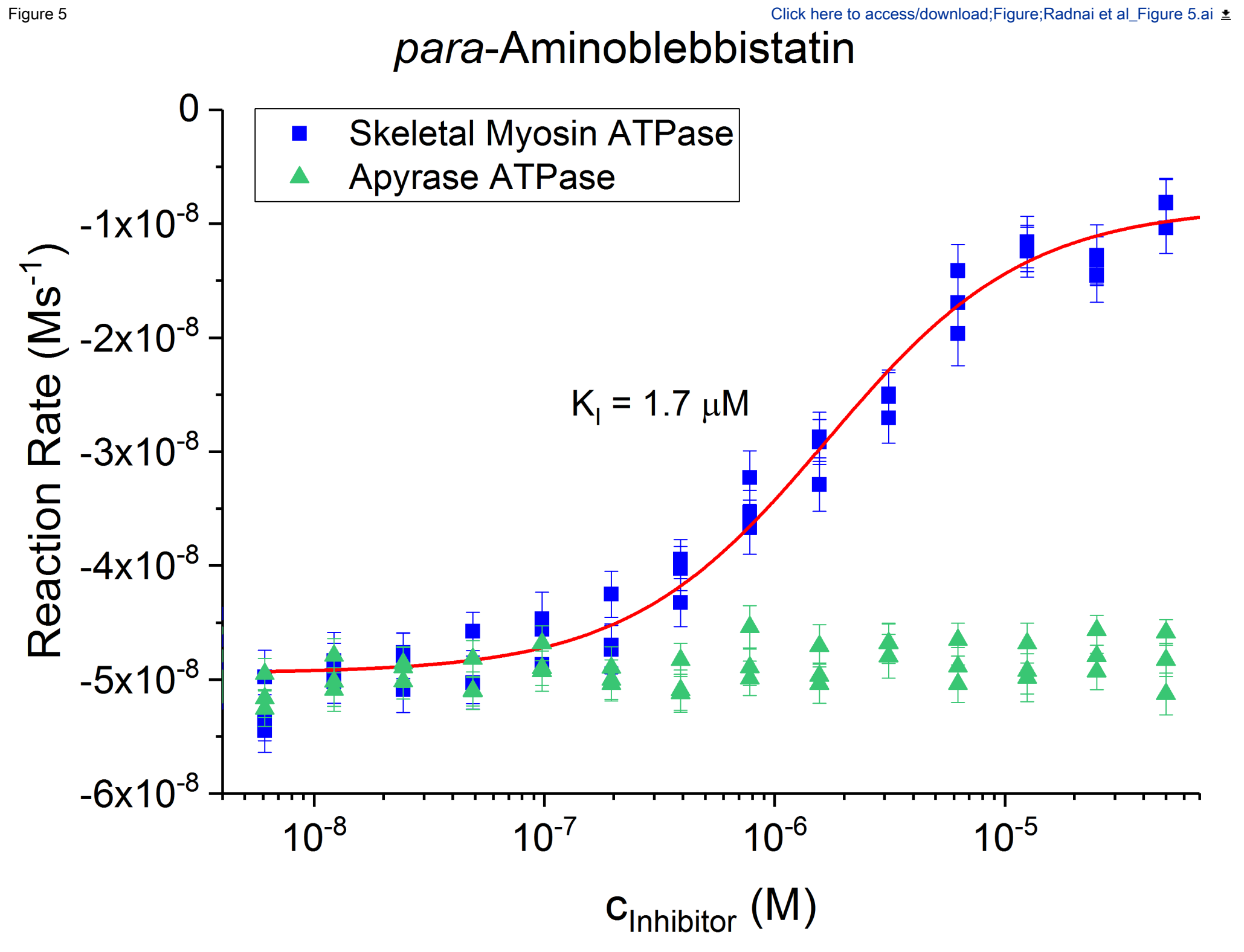

Name of Material/Equipment	Company	Catalog Number
384-well Low Flange Black Flat Bottom Polystyrene NBS Microplate	Corning	3575
ATP (Adenosine 5'-triphosphate disodium salt hydrate)	Sigma	A7699
Aurora FRD-IB Dispenser	Aurora Discovery, Inc.	00017425
Biomek NXP Multichannel Laboratory Automation Workstation	Beckman Coulter	A31841
Blebbistatin	AMRI	N/A
BSA (Bovine Serum Albumin, Protease-Free)	Akron Biotech	AK1391
Centrifuge 5430 R, refrigerated, with Rotor FA-35-6-30	Eppendorf	022620663
Centrifuge 5430, non-refrigerated, with Rotor A-2-MTP	Eppendorf	022620568
DMSO (Dimethyl sulfoxide)	Sigma	D2650
DTT (DL-Dithiothreitol)	Sigma	D5545
E1 ClipTip Multichannel Pipette; 384-format; 8-channel	Thermo Scientific	4672010
E1 ClipTip Multichannel Pipette; 96-format; 8-channel	Thermo Scientific	4672080
EGTA (Ethylene glycol-bis(2-aminoethylether)-N,N,N',N'-tetraacetic acid)	Sigma	E3889
EnVision 2104 Multilabel Plate Reader	PerkinElmer	2104-0010
Glycerol	Sigma	G2025
LDH (L-Lactic Dehydrogenase from rabbit muscle)	Sigma	L1254
$MgCl_2.6H_2O$ (Magnesium chloride hexahydrate)	Sigma	M2670
Microplate Shaker	VWR	12620-926
Microplate, 384 well, PP, Small Volume, Deep Well, Natural	Greiner Bio-One	784201
MOPS (3-(N-Morpholino)propanesulfonic acid)	Sigma	M1254
Myosin Motor Protein (full length) (Bovine cardiac muscle)	Cytoskeleton	MY03
Myosin Motor Protein (full length) (Rabbit skeletal muscle)	Cytoskeleton	MY02
NADH (β-Nicotinamide adenine dinucleotide, reduced disodium salt hydrate)	Sigma	N8129
NaN_3 (Sodium azide)	Sigma	71289
NaOH (Sodium hydroxide)	Sigma	S8045
Optical Filter CFP 470/24nm (Emission)	PerkinElmer	2100-5850
Optical Filter Fura2 380/10nm (Excitation)	PerkinElmer	2100-5390
Optical Module: Beta Lactamase	PerkinElmer	2100-4270
OriginPro 2017 software	OriginLab	N/A
para- Aminoblebbistatin	AMRI	N/A
para- Nitroblebbistatin	AMRI	N/A
PEP (Phospho(enol)pyruvic acid monopotassium salt)	Sigma	P7127

PK (Pyruvate Kinase from rabbit muscle)	Sigma	P9136
Rabbit Muscle Acetone Powder	Pel Freez Biologicals	41995-2

Comments/Description

Custom synthesis

Barcode 240
Barcode 112
Barcode 418

Custom synthesis
Custom synthesis

jove JOURNAL OF VISUALIZED EXPERIMENTS
1 Alewife Center #200
Cambridge, MA 02140
tel. 617.945.9051
www.jove.com

ARTICLE AND VIDEO LICENSE AGREEMENT

Title of Article: A semi-high-throughput adaptation of the NADH-coupled ATPase assay for screening small molecule inhibitors

Author(s): Laszlo Radnai, Rebecca Stremel, James Seilers, Gavin Rumbaugh and Courtney Miller

Item 1: The Author elects to have the Materials be made available (as described at http://www.jove.com/publish) via:

☑ Standard Access ☐ Open Access

Item 2: Please select one of the following items:

☑ The Author is **NOT** a United States government employee.

☐ The Author is a United States government employee and the Materials were prepared in the course of his or her duties as a United States government employee.

☐ The Author is a United States government employee but the Materials were NOT prepared in the course of his or her duties as a United States government employee.

ARTICLE AND VIDEO LICENSE AGREEMENT

1. **Defined Terms.** As used in this Article and Video License Agreement, the following terms shall have the following meanings: "**Agreement**" means this Article and Video License Agreement; "**Article**" means the article specified on the last page of this Agreement, including any associated materials such as texts, figures, tables, artwork, abstracts, or summaries contained therein; "**Author**" means the author who is a signatory to this Agreement; "**Collective Work**" means a work, such as a periodical issue, anthology or encyclopedia, in which the Materials in their entirety in unmodified form, along with a number of other contributions, constituting separate and independent works in themselves, are assembled into a collective whole; "**CRC License**" means the Creative Commons Attribution-Non Commercial-No Derivs 3.0 Unported Agreement, the terms and conditions of which can be found at: http://creativecommons.org/licenses/by-nc-nd/3.0/legalcode; "**Derivative Work**" means a work based upon the Materials or upon the Materials and other pre-existing works, such as a translation, musical arrangement, dramatization, fictionalization, motion picture version, sound recording, art reproduction, abridgment, condensation, or any other form in which the Materials may be recast, transformed, or adapted; "**Institution**" means the institution, listed on the last page of this Agreement, by which the Author was employed at the time of the creation of the Materials; "**JoVE**" means MyJove Corporation, a Massachusetts corporation and the publisher of The Journal of Visualized Experiments; "**Materials**" means the Article and / or the Video; "**Parties**" means the Author and JoVE; "**Video**" means any video(s) made by the Author, alone or in conjunction with any other parties, or by JoVE or its affiliates or agents, individually or in collaboration with the Author or any other parties, incorporating all or any portion of the Article, and in which the Author may or may not appear.

2. **Background.** The Author, who is the author of the Article, in order to ensure the dissemination and protection of the Article, desires to have the JoVE publish the Article and create and transmit videos based on the Article. In furtherance of such goals, the Parties desire to memorialize in this Agreement the respective rights of each Party in and to the Article and the Video.

3. **Grant of Rights in Article.** In consideration of JoVE agreeing to publish the Article, the Author hereby grants to JoVE, subject to **Sections 4** and **7** below, the exclusive, royalty-free, perpetual (for the full term of copyright in the Article, including any extensions thereto) license (a) to publish, reproduce, distribute, display and store the Article in all forms, formats and media whether now known or hereafter developed (including without limitation in print, digital and electronic form) throughout the world, (b) to translate the Article into other languages, create adaptations, summaries or extracts of the Article or other Derivative Works (including, without limitation, the Video) or Collective Works based on all or any portion of the Article and exercise all of the rights set forth in (a) above in such translations, adaptations, summaries, extracts, Derivative Works or Collective Works and(c) to license others to do any or all of the above. The foregoing rights may be exercised in all media and formats, whether now known or hereafter devised, and include the right to make such modifications as are technically necessary to exercise the rights in other media and formats. If the "Open Access" box has been checked in **Item 1** above, JoVE and the Author hereby grant to the public all such rights in the Article as provided in, but subject to all limitations and requirements set forth in, the CRC License.

4. **Retention of Rights in Article.** Notwithstanding the exclusive license granted to JoVE in **Section 3** above, the Author shall, with respect to the Article, retain the non-exclusive right to use all or part of the Article for the non-commercial purpose of giving lectures, presentations or teaching classes, and to post a copy of the Article on the Institution's website or the Author's personal website, in each case provided that a link to the Article on the JoVE website is provided and notice of JoVE's copyright in the Article is included. All non-copyright intellectual property rights in and to the Article, such as patent rights, shall remain with the Author.

5. **Grant of Rights in Video – Standard Access.** This **Section 5** applies if the "Standard Access" box has been checked in **Item 1** above or if no box has been checked in **Item 1** above. In consideration of JoVE agreeing to produce, display or otherwise assist with the Video, the Author hereby acknowledges and agrees that, Subject to **Section 7** below, JoVE is and shall be the sole and exclusive owner of all rights of any nature, including, without limitation, all copyrights, in and to the Video. To the extent that, by law, the Author is deemed, now or at any time in the future, to have any rights of any nature in or to the Video, the Author hereby disclaims all such rights and transfers all such rights to JoVE.

6. **Grant of Rights in Video – Open Access.** This **Section 6** applies only if the "Open Access" box has been checked in **Item 1** above. In consideration of JoVE agreeing to produce, display or otherwise assist with the Video, the Author hereby grants to JoVE, subject to **Section 7** below, the exclusive, royalty-free, perpetual (for the full term of copyright in the Article, including any extensions thereto) license (a) to publish, reproduce, distribute, display and store the Video in all forms, formats and media whether now known or hereafter developed (including without limitation in print, digital and electronic form) throughout the world, (b) to translate the Video into other languages, create adaptations, summaries or extracts of the Video or other Derivative Works or Collective Works based on all or any portion of the Video and exercise all of the rights set forth in (a) above in such translations, adaptations, summaries, extracts, Derivative Works or Collective Works and (c) to license others to do any or all of the above. The foregoing rights may be exercised in all media and formats, whether now known or hereafter devised, and include the right to make such modifications as are technically necessary to exercise the rights in other media and formats. For any Video to which this **Section 6** is applicable, JoVE and the Author hereby grant to the public all such rights in the Video as provided in, but subject to all limitations and requirements set forth in, the CRC License.

7. **Government Employees.** If the Author is a United States government employee and the Article was prepared in the course of his or her duties as a United States government employee, as indicated in **Item 2** above, and any of the licenses or grants granted by the Author hereunder exceed the scope of the 17 U.S.C. 403, then the rights granted hereunder shall be limited to the maximum rights permitted under such statute. In such case, all provisions contained herein that are not in conflict with such statute shall remain in full force and effect, and all provisions contained herein that do so conflict shall be deemed to be amended so as to provide to JoVE the maximum rights permissible within such statute.

8. **Protection of the Work.** The Author(s) authorize JoVE to take steps in the Author(s) name and on their behalf if JoVE believes some third party could be infringing or might infringe the copyright of either the Author's Article and/or Video.

9. **Likeness, Privacy, Personality.** The Author hereby grants JoVE the right to use the Author's name, voice, likeness, picture, photograph, image, biography and performance in any way, commercial or otherwise, in connection with the Materials and the sale, promotion and distribution thereof. The Author hereby waives any and all rights he or she may have, relating to his or her appearance in the Video or otherwise relating to the Materials, under all applicable privacy, likeness, personality or similar laws.

10. **Author Warranties.** The Author represents and warrants that the Article is original, that it has not been published, that the copyright interest is owned by the Author (or, if more than one author is listed at the beginning of this Agreement, by such authors collectively) and has not been assigned, licensed, or otherwise transferred to any other party. The Author represents and warrants that the author(s) listed at the top of this Agreement are the only authors of the Materials. If more than one author is listed at the top of this Agreement and if any such author has not entered into a separate Article and Video License Agreement with JoVE relating to the Materials, the Author represents and warrants that the Author has been authorized by each of the other such authors to execute this Agreement on his or her behalf and to bind him or her with respect to the terms of this Agreement as if each of them had been a party hereto as an Author. The Author warrants that the use, reproduction, distribution, public or private performance or display, and/or modification of all or any portion of the Materials does not and will not violate, infringe and/or misappropriate the patent, trademark, intellectual property or other rights of any third party. The Author represents and warrants that it has and will continue to comply with all government, institutional and other regulations, including, without limitation all institutional, laboratory, hospital, ethical, human and animal treatment, privacy, and all other rules, regulations, laws, procedures or guidelines, applicable to the Materials, and that all research involving human and animal subjects has been approved by the Author's relevant institutional review board.

11. **JoVE Discretion.** If the Author requests the assistance of JoVE in producing the Video in the Author's facility, the Author shall ensure that the presence of JoVE employees, agents or independent contractors is in accordance with the relevant regulations of the Author's institution. If more than one author is listed at the beginning of this Agreement, JoVE may, in its sole

jove JOURNAL OF VISUALIZED EXPERIMENTS
1 Alewife Center #200
Cambridge, MA 02140
tel. 617.945.9051
www.jove.com

ARTICLE AND VIDEO LICENSE AGREEMENT

discretion, elect not take any action with respect to the Article until such time as it has received complete, executed Article and Video License Agreements from each such author. JoVE reserves the right, in its absolute and sole discretion and without giving any reason therefore, to accept or decline any work submitted to JoVE. JoVE and its employees, agents and independent contractors shall have full, unfettered access to the facilities of the Author or of the Author's institution as necessary to make the Video, whether actually published or not. JoVE has sole discretion as to the method of making and publishing the Materials, including, without limitation, to all decisions regarding editing, lighting, filming, timing of publication, if any, length, quality, content and the like.

12. **Indemnification.** The Author agrees to indemnify JoVE and/or its successors and assigns from and against any and all claims, costs, and expenses, including attorney's fees, arising out of any breach of any warranty or other representations contained herein. The Author further agrees to indemnify and hold harmless JoVE from and against any and all claims, costs, and expenses, including attorney's fees, resulting from the breach by the Author of any representation or warranty contained herein or from allegations or instances of violation of intellectual property rights, damage to the Author's or the Author's institution's facilities, fraud, libel, defamation, research, equipment, experiments, property damage, personal injury, violations of institutional, laboratory, hospital, ethical, human and animal treatment, privacy or other rules, regulations, laws, procedures or guidelines, liabilities and other losses or damages related in any way to the submission of work to JoVE, making of videos by JoVE, or publication in JoVE or elsewhere by JoVE. The Author shall be responsible for, and shall hold JoVE harmless from, damages caused by lack of sterilization, lack of cleanliness or by contamination due to the making of a video by JoVE its employees, agents or independent contractors. All sterilization, cleanliness or decontamination procedures shall be solely the responsibility of the Author and shall be undertaken at the Author's expense. All indemnifications provided herein shall include JoVE's attorney's fees and costs related to said losses or damages. Such indemnification and holding harmless shall include such losses or damages incurred by, or in connection with, acts or omissions of JoVE, its employees, agents or independent contractors.

13. **Fees.** To cover the cost incurred for publication, JoVE must receive payment before production and publication the Materials. Payment is due in 21 days of invoice. Should the Materials not be published due to an editorial or production decision, these funds will be returned to the Author. Withdrawal by the Author of any submitted Materials after final peer review approval will result in a US$1,200 fee to cover pre-production expenses incurred by JoVE. If payment is not received by the completion of filming, production and publication of the Materials will be suspended until payment is received.

14. **Transfer, Governing Law.** This Agreement may be assigned by JoVE and shall inure to the benefits of any of JoVE's successors and assignees. This Agreement shall be governed and construed by the internal laws of the Commonwealth of Massachusetts without giving effect to any conflict of law provision thereunder. This Agreement may be executed in counterparts, each of which shall be deemed an original, but all of which together shall be deemed to me one and the same agreement. A signed copy of this Agreement delivered by facsimile, e-mail or other means of electronic transmission shall be deemed to have the same legal effect as delivery of an original signed copy of this Agreement.

A signed copy of this document must be sent with all new submissions. Only one Agreement is required per submission.

CORRESPONDING AUTHOR

Name:	Courtney Miller
Department:	Molecular Medicine
Institution:	The Scripps Research Institute
Title:	Associate Professor
Signature:	Courtney Miller
Date:	3/20/19

Please submit a **signed** and **dated** copy of this license by one of the following three methods:

1. Upload an electronic version on the JoVE submission site
2. Fax the document to +1.866.381.2236
3. Mail the document to JoVE / Attn: JoVE Editorial / 1 Alewife Center #200 / Cambridge, MA 02140

Courtney A. Miller, Ph.D.

Associate Professor
Department of Molecular Medicine
Department of Neuroscience
Scripps Research
130 Scripps Way, 3B3
Jupiter, FL 33458
Tel: 561-228-2958
Email: cmiller@scripps.edu
Website: www.scripps.edu

We are pleased to submit a revised version of our manuscript, "*A semi-high-throughput adaptation of the NADH-coupled ATPase assay for screening small molecule inhibitors*".

We thank the editor and reviewers for their constructive comments, as well as the time and effort put into the review of the manuscript. We have considered the reviewer's comments carefully and have accordingly revised the manuscript. Responses to the comments from the reviewers can be found below and the revised manuscript accompanies this letter, with changes indicated in a teal font. We hope the revised version is now suitable for publication and look forward to hearing from you.

Editor Comments:

1. Please take this opportunity to thoroughly proofread the manuscript to ensure that there are no spelling or grammar issues.

Complete.

2. Please obtain explicit copyright permission to reuse any figures from a previous publication. Explicit permission can be expressed in the form of a letter from the editor or a link to the editorial policy that allows re-prints. Please upload this information as a .doc or .docx file to your Editorial Manager account. The Figure must be cited appropriately in the Figure Legend, i.e. "This figure has been modified from [citation]."

Not applicable.

3. Please use greek characters for SI unit prefixed, e.g. use 'µM' instead of 'uM'.

Complete.

4. Please do not abbreviate journal titles for references.

We have followed the format in published JoVE reference lists and used the JoVE Endnote format.

5. JoVE cannot publish manuscripts containing commercial language. This includes company names of an instrument or reagent. Please remove all commercial language from your manuscript and use generic terms instead. All commercial products should be sufficiently referenced in the Table of Materials and Reagents. Examples of commercial language in your manuscript include Milli-Q, etc.

Complete.

Reviewer 1:

Manuscript Summary:
This manuscript gives a good, detailed overview of a high-throughput miniaturised version of the classical NADH-enzyme coupled ATPase assay. Examples are given using myosin and ATPase inhibitors. The protocol is well written and easy to follow. This will be a benefit to the community and the benefits of this approach versus other methods are discussed.

Minor Concerns:

1. The addition of ADP would drive the change in signal to ensure PK/LDH is working correctly in the presence of the inhibitors. It would be useful to add a statement to this effect.

We fully agree with the reviewer that the above described experiment is an important control and may help users during troubleshooting. The following paragraph has been added to the Discussion (pg. 9, Line 481-487): "It is important to ensure that the reaction catalyzed by PK and LDH are not rate limiting in the coupled reaction system. Control experiments performed without the ATPase of interest or at high levels of a potent ATPase inhibitor would show no (or little) activity, however, the addition of ADP would result in a quick signal decrease if LDH and PK are active and work correctly. The rate of NADH consumption is expected to be very high in this control experiment, so it is crucial to start detection as soon as possible after the reaction has been initiated by the addition of ADP."

Reviewer #2:

Manuscript Summary:
This manuscript describes a method for using a well-established but often challenging and problematic assay. Inconsistencies are often common when running this assay so it will be very helpful to many scientists to have a highly detailed protocol that also includes a list of trouble spots and key procedures to follow to gain the most repeatable and valid results. The authors also very nicely explain the advantages of this method versus the other common methods.

Minor Concerns:

1. It would be nice to see the data reported in the conventional value of per second/per myosin head. Most articles that use this technique report their findings in this value so that would be helpful.

Although we fully agree with the reviewer that many publications show ATPase data as per second/per ATPase enzyme and it may help readers to make comparisons across papers or enzymes, we prefer using "raw" ATP (NADH) consumption rates here for several reasons. First, the observed NADH consumption rate does not purely reflect the ATP consumption rate of myosin, but it is affected by the photochemical degradation of NADH, the spontaneous hydrolysis of ATP, and the presence of any other ATPase enzymes. Besides the potential presence of contaminant ATPases, the slow ATPase activity of actin is the most important factor in this case. Therefore, uncorrected ATPase rates expressed as per second/per myosin head could be misleading. The best way to perform correction is to subtract the estimated reaction rate at 100% myosin inhibition from the data, which can only be performed after the inhibitory constants has been estimated by fitting the appropriate equation to the dose-response data. These extra steps of correction and further transformation would complicate the manuscript and, therefore, may not benefit the manuscript's goal of presenting a straightforward protocol describing how screening is performed, the raw data is analyzed, and the performance (potency) of compounds is evaluated. However, we are willing to include the data in this format if the Reviewer feels strongly.

2. It would also be helpful to describe how the potential differences are quantified. E.g. is a 95% C.I. created around the slopes and then compared across the drugs? Or is an ANOVA run on a point by point basis. Which would be best for the researcher to use?

We appreciate that the reviewer has highlighted the importance of addressing statistical evaluation of differences between compound potencies. The following two paragraphs have been added to the manuscript to give practical hints to the readers (pgs. 10-11, Lines 521-539):

"Differences in compound potencies should always be quantified by performing dose-response experiments and determining the inhibitory constants. Although single point screening data reflects these differences in theory, the non-linearity of the responses, together with the experimental error would make it extremely difficult to perform such an analysis. Single point screening experiments should be designed to capture even the relatively weak inhibitors with high confidence by choosing an appropriate inhibitor concentration and a pre-defined threshold response level to distinguish between active and inactive compounds."

"Establishing that the differences between the inhibitory constants are statistically significant is best performed by re-writing the equation for nonlinear regression to determine pK_I ($-\log K_I$) instead of K_I, as pK_I is normally distributed, while K_I is not. The uncertainty for pK_I is symmetrical, while it is not symmetrical for K_I. Confidence intervals can be calculated for pK_I and t-test or ANOVA can be used to determine if the means of pK_I measurements are significantly different. However, caution must be taken when performing such statistical test as they assume homoscedasticity (same variance of data in groups). One can expect higher variance associated with pK_I when a full dose-response curve cannot be obtained due to compound solubility issues. In this case, other appropriate statistical tests not assuming equal variances (e.g. Welch's t-test) should be used."

3. The method for assessing if a small molecule might affect the other enzymes of the assay is nicely detailed (lines 444-450). Is this describing how to interpret the negative and positive controls in Figure 2F? It might be helpful to make this clearer in the text as it seems a very important control when interested in small molecules that might affect LDH and PK as well as myosin, or the enzyme of interest.

This is an excellent point and we have included new data to address it. *Para*-Aminoblebbistain is a known myosin inhibitor. It has been used as a positive control (dissolved in DMSO), while DMSO containing no inhibitor was used as a negative control throughout this work, as shown in Fig. 2F. To demonstrate that *para*-aminoblebbistain is indeed a good positive control that inhibits myosin, but does not affect LDH and PK, the same ATPase assay was performed by using apyrase instead of myosin. Apyrase hydrolyses ATP to yield ADP and inorganic phosphate. As expected, *para*-aminoblebbistain was inactive in this assay, showing that the inhibition in the case of the myosin ATPase assay is not related to the loss of LDH or PK activity, but to the binding and inhibition of myosin by *para*-aminoblebbistain. A new figure (Fig. 5) and the following paragraph have been included in the revision to clarify the details of this control experiment (pg. 7, Line 380-386):

"Finally, it is always recommended to test whether the inhibitory effects of any positive hits are specific to the target ATPase enzyme. The coupled reaction system employs two other enzymes, LDH and PK, and inhibition of one of these would result in a false positive signal. Running the ATPase assay with an unrelated ATPase enzyme may help to filter out these false positive hits. (For further recommendations, see discussion.) *Para*-aminoblebbistatin and apyrase, an ATP hydrolyzing enzyme producing ADP and inorganic phosphate, were used here as an example to demonstrate such a control experiment, as shown in **Figure 5**."

The corresponding paragraph in the Discussion (pg. 11, Lines 543-548) has also been modified to indicate these changes and to further clarify what other control experiments can be performed.

Figure 1

Click here to access/download;Supplemental File (Figures, Permissions, etc.);Radnai et al_Figure 1.tif

Your image file "Radnai et al_Figure 1.tif" cannot be opened and processed. Please see the common list of problems, and suggested resolutions below.

Reason: The image file is corrupt or invalid. Please check and resubmit.

Other Common Problems When Creating a PDF from an image file

You will need to convert your image file to another format or fix the current image, then re-submit it.

Figure 2

Click here to access/download;Supplemental File (Figures, Permissions, etc.);Radnai et al_Figure 2.psd

Your image file "Radnai et al_Figure 2.psd" cannot be opened and processed. Please see the common list of problems, and suggested resolutions below.

Reason: The image file is corrupt or invalid. Please check and resubmit.

Other Common Problems When Creating a PDF from an image file

You will need to convert your image file to another format or fix the current image, then re-submit it.

Figure 3

Click here to access/download;Supplemental File (Figures, Permissions, etc.);Radnai et al_Figure 3.psd

Your image file "Radnai et al_Figure 3.psd" cannot be opened and processed. Please see the common list of problems, and suggested resolutions below.

Reason: The image file is corrupt or invalid. Please check and resubmit.

Other Common Problems When Creating a PDF from an image file

You will need to convert your image file to another format or fix the current image, then re-submit it.

Figure 4

Click here to access/download;Supplemental File (Figures, Permissions, etc.);Radnai et al_Figure 4.psd

Your image file "Radnai et al_Figure 4.psd" cannot be opened and processed. Please see the common list of problems, and suggested resolutions below.

Reason: The image file is corrupt or invalid. Please check and resubmit.

Other Common Problems When Creating a PDF from an image file

You will need to convert your image file to another format or fix the current image, then re-submit it.

Figure 5

Click here to access/download;Supplemental File (Figures, Permissions, etc.);Radnai et al_Figure 5.psd

Your image file "Radnai et al_Figure 5.psd" cannot be opened and processed. Please see the common list of problems, and suggested resolutions below.

Reason: The image file is corrupt or invalid. Please check and resubmit.

Other Common Problems When Creating a PDF from an image file

You will need to convert your image file to another format or fix the current image, then re-submit it.